



## Embrittlement and aging at 475 °C in an experimental superferritic stainless steel with high molybdenum content



Lorena Braga Moura<sup>a,\*</sup>, Hamilton Ferreira Gomes de Abreu<sup>b</sup>, Walney Silva Araújo<sup>c</sup>,  
João Felipe Bastos Franco<sup>a</sup>, Michael Carneiro Sampaio<sup>a</sup>, Francisco Eric Rodrigues Maurício<sup>a</sup>

<sup>a</sup> Mechanical Test Laboratory, Instituto Federal de Educação, Ciências e Tecnologia do Ceará, Department of Industry, Fortaleza, CE, CEP:60.040215, Brazil

<sup>b</sup> Materials Characterization Laboratory, Universidade Federal do Ceará, Department of Metallurgical and Materials Engineering, Fortaleza, CE, CEP:60.455760, Brazil

<sup>c</sup> Corrosion Laboratory, Universidade Federal do Ceará, Department of Metallurgical and Materials Engineering, Fortaleza, CE, CEP:60.455760, Brazil

### ARTICLE INFO

#### Keywords:

Superferritic stainless steel  
High molybdenum  
Embrittlement

### ABSTRACT

Superferritic steels are characterized by high Cr content (exceeding 25 wt.%) with addition of Mo. They were originally developed for use in heat exchangers and marine environments. Current trend to use these alloys in the oil industry drives the research on effect of the increased Mo content on the microstructure of these steels. Mo increases the resistance to naphthenic corrosion. The  $\alpha'$  (alpha prime) phase precipitation, typical in Fe-Cr system, causes Cr depletion in the ferritic matrix which decreases the corrosion resistance, toughness and increases hardness of steels. This phase is rich in Cr, has paramagnetic properties and occurs in the temperature range between 350 and 550 °C. The influence of increase of Mo content and Ni addition is investigated in the temperature range of  $\alpha'$  phase precipitation in experimental Superferritic stainless steel FeCrMoNi with different compositions. An initial analysis was performed with Thermo-Calc® (TCFE6). Samples were subjected to aging treatment for different time and temperatures. Results of micro hardness tests, magnetic measurements (by means of ferritoscope) and corrosion test, were used to study the precipitation behaviour of  $\alpha'$  phase. The results were compared with solution annealed samples and results obtained from the Thermo-Calc® calculation.

### 1. Introduction

Superferritic stainless steels (SFSS) are widely used in applications where chloride induced pitting, crevice, and stress corrosion cracking are present. They present a lower fabrication cost when compared to super austenitic stainless steels. These alloys can be used in many corrosive environments, for example, in chemical industries, petroleum refineries, petrochemical industries, food and paper industries, in heat condensers for seawater, and other marine applications [1,5].

They generally have superior corrosion resistance to their austenitic counterparts because of their higher Cr contents and ferritic microstructures; however, the use of SFSS has been somewhat limited by poor weldability and low toughness in certain applications [3–7].

The increase in the performance of ferritic stainless steels is achieved with levels of Cr above 25% and Mo additions. Studies have been published that Mo addition improves corrosion resistance in various corrosive environments including naphthenic acid corrosion that results from the processing of heavy crude oil [8–12]. The low levels of C and N improve the ductility and corrosion resistance, and allow the addition of Ni to

improve the toughness. Also, the addition of stabilizing elements such as Nb and Ti hinder the formation of carbides and nitrides and act in the grain refinement and improve weldability [2,5,7,13–15].

The high concentration of alloying elements in stainless steels affects the microstructural stability resulting in precipitation of intermetallic phases (Sigma- $\sigma$ , Mu- $\mu$ , Chi- $\chi$  and Laves) [15–18]. The phenomenon of embrittlement at 475 °C is due to precipitation of  $\alpha'$  phase resulting chromium depletion in the matrix [19–21]. The  $\alpha'$  phase is rich in chromium, CrFe (61–83% Cr), with BCC structure, precipitates in a temperature range between 350 °C and 550 °C. The precipitates are extremely small and their presence is accompanied by an increase in hardness, loss in corrosion resistance and reduced toughness [20–23]. The  $\alpha'$  phase can be formed from two mechanisms: nucleation and growth and spinodal decomposition of the ferrite ( $\alpha \rightarrow \alpha + \alpha'$ ) [19,20]. The decrease in the volume fraction of ferrite phase ( $\alpha$ ) suggests the formation of  $\alpha'$  phase which is a paramagnetic phase. Several authors have noted that ferritic stainless steel for the study of  $\alpha'$  precipitation stage based on the magnetic permeability may be feasible for samples heat treated at 400 °C and 475 °C [22–25]. The precipitation  $\alpha'$  phase in the ferritic matrix inhibits

\* Corresponding author.

E-mail addresses: [lorenabraga@ifce.edu.br](mailto:lorenabraga@ifce.edu.br) (L.B. Moura), [hamilton@ufc.br](mailto:hamilton@ufc.br) (H.F.G. de Abreu), [wsa@ufc.br](mailto:wsa@ufc.br) (W.S. Araújo), [felipefrancobt@gmail.com](mailto:felipefrancobt@gmail.com) (J.F.B. Franco), [michaelc.s@hotmail.com](mailto:michaelc.s@hotmail.com) (M.C. Sampaio), [ericmauricio2010@hotmail.com](mailto:ericmauricio2010@hotmail.com) (F.E.R. Maurício).

<https://doi.org/10.1016/j.corsci.2018.03.033>

Received 3 March 2017; Received in revised form 14 March 2018; Accepted 16 March 2018

Available online 04 April 2018

0010-938X/ © 2018 Elsevier Ltd. All rights reserved.

**Table 1**  
Chemical Composition (in weight percent) of experimental alloys and value of PRE.

Alloys	Cr	Mo	Ni	C	N	Nb + Ti	PRE
5Mo4Ni	25	5	4	0,03	0,03	0,6	41,98
7Mo2Ni	25	7	2	0,03	0,03	0,6	48,58
7Mo4Ni	25	7	4	0,03	0,03	0,6	48,58

**Table 2**  
Thermal processing of samples.

Alloys	Solubilization Temperature (°C)	Solubilization Time (min)	Aging Temperature (°C)	Aging Time (h)
5Mo4Ni	1080	15	–	1 h, 10 h,
7Mo2Ni	1180	15	400 and 475	100 h,
				500 h,
7Mo4Ni	1180	15	–	1000 h

movement and the rotation of the magnetic fields, requiring a larger external field inducer to move the walls of the magnetic domains, causing a decrease in magnetic permeability, defined as the ratio between magnetic induction and applied field [22,23].

The depletion of Cr in the matrix decreases corrosion resistance and increases the susceptibility to pitting corrosion. Pitting corrosion is highly localized, causes the formation of small holes or points on the surface of the component, has a high propagation rate, and can be completely destructive in terms of useful life of the component [22,23]. The pitting resistance equivalent (PRE) for stainless steels is often expressed in terms of Eq. (1), developed by Rockel in 1978 and tested by the ASTM G 48-99 [1].

This work studies the effect of precipitation of the  $\alpha'$  phase in SFSS new alloys with high content of Mo and Ni addition. Changes in hardness, magnetic behavior, corrosion resistance and X-ray diffraction measurements in aged and solution annealed samples are compared with Thermo-Calc analysis.

## 2. Materials and methods

FeCrMoNi experimental alloys containing 25% Cr, Ni content of 2% and 4%, Mo content of 5 and 7% were studied. Table 1 shows the

chemical composition of experimental alloys and the value of PRE calculated according to Eq. (1).

The thermodynamic analysis of the alloys was performed with the Thermo-Calc (TCFE6 database) software. It was evaluated the influence of the variation of the Mo and Ni contents in the precipitation temperature of  $\alpha'$  phase. Based on this analysis the samples were solution annealed and heat treated at temperatures of 400 °C and 475 °C for various times according to Table 2.

The effects of thermal processing comparing the samples annealed with aged were observed through measurements of X-ray diffraction (XRD), CuK $\alpha$  source and 0.01° step 2 $\theta$ , used to identify the possible precipitated phases. Vickers micro hardness (HV) measurements, with 9,8N load, were performed to observe the changes in hardness due to phases precipitation. Ferritoscope measurements based on the variations of magnetic permeability of the ferrite phase were used to evaluate the paramagnetic phase precipitation ( $\alpha'$  phase). Ferritoscope measurement is performed when a magnetic field generated by a coil interacts with the magnetic phase of the sample. Changes in the magnetic field induce a voltage proportional to the content of the ferromagnetic phase in a second coil. This output voltage is then evaluated. The output signal of ferritoscope is proportional to the ferromagnetic phase content of the sample [24].

Polarization tests were conducted in 0.6 M NaCl aqueous solution at room temperature (25 °C) with a reference electrode Ag/AgCl and platinum counter electrode. It was evaluated the corrosion resistance of aged samples for 1000 h compared to solution annealed samples. The effect of corrosion tests on the sample surface were observed by scanning electron microscopy (SEM).

## 3. Results and discussion

### 3.1. Computational thermodynamic analysis

The data of the phase diagram FeCr, calculated in Thermo-Calc software, with gradual Mo addition (without Ni) were used to relate the precipitation temperature of  $\alpha'$  phase with Mo content. Fig. 1 illustrates the influence of the Mo content in the precipitation temperature of  $\alpha'$  phase. Mo addition reduces the temperature range in which occurs  $\alpha'$  phase precipitation. For an alloy with 25 wt.% of Cr and 0% of Mo  $\alpha'$  phase can exist until approximately 520 °C. This limit is the beginning of precipitation of  $\sigma$  (sigma) phase in thermodynamic equilibrium conditions [15]. The Mo addition decreases such temperature to about 400 °C in the alloy with 25% of Cr and 7% of Mo.

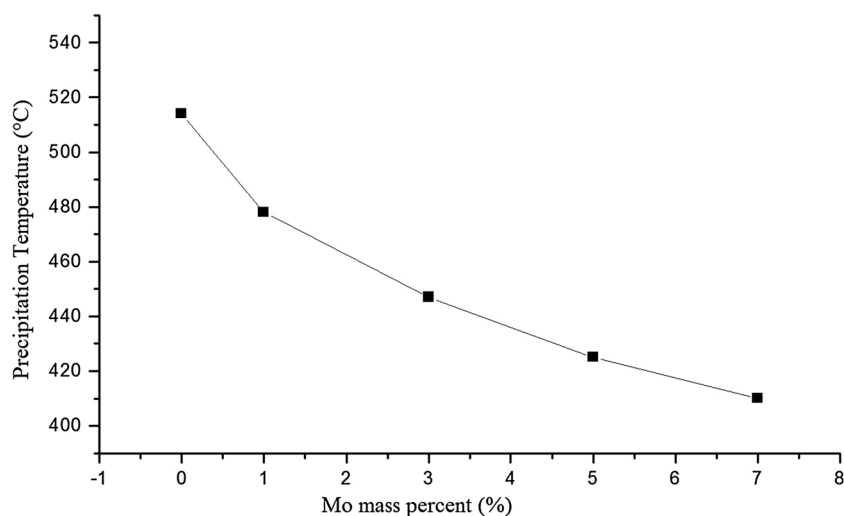


Fig. 1.  $\alpha'$  phase precipitation temperature as a function of wt.% of Mo for FeCr alloys.

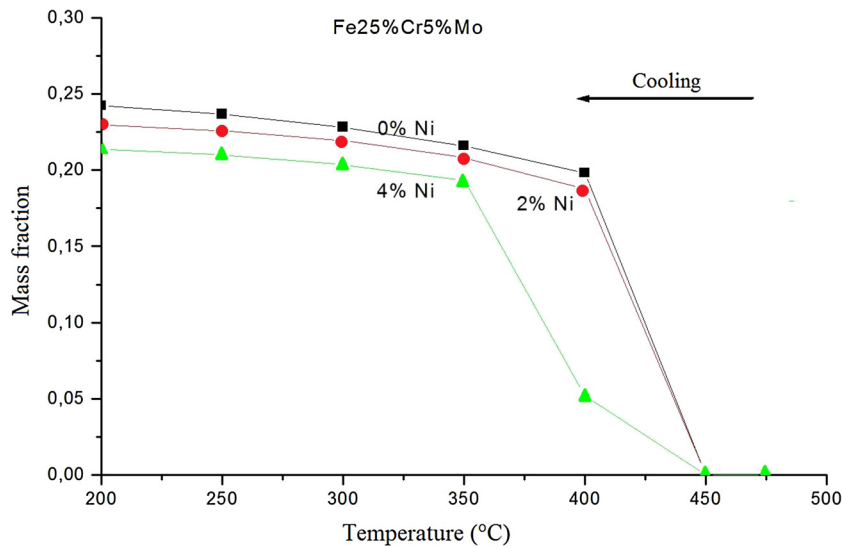


Fig. 2.  $\alpha'$  phase mass fraction as a function of temperature and %Ni for Fe25%Cr5%Mo system.

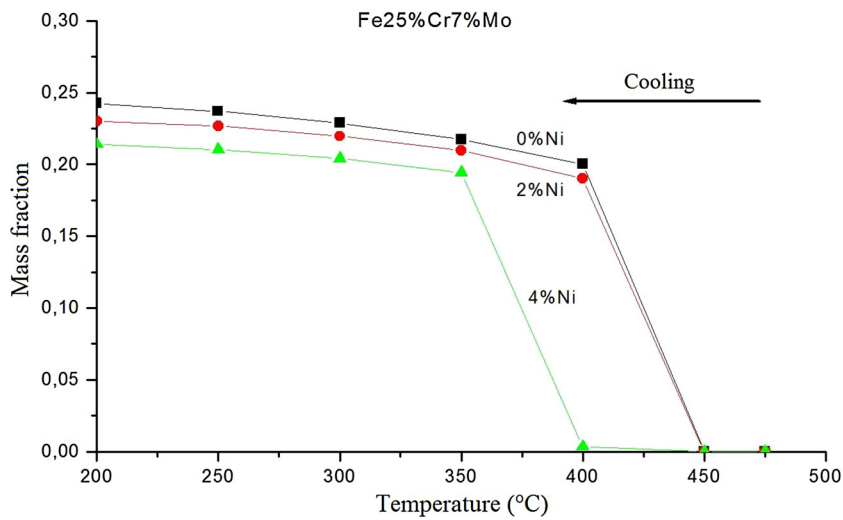


Fig. 3.  $\alpha'$  phase mass fraction as a function of temperature and %Ni for Fe25%Cr7%Mo system.

Figs. 2 and 3 show the mass fraction of the  $\alpha'$  phase as a function of the of Mo and Ni content in the Fe 25% Cr system. Mo addition increases the amount of  $\alpha'$  phase. The Ni addition reduces the mass fraction of  $\alpha'$  phase. The precipitation temperature range of the  $\alpha'$  phase does not change with the Ni addition. Based on Thermo-Calc calculations at 450 °C does not exist  $\alpha'$  phase in thermodynamic equilibrium conditions. Aging treatments at 400 °C and 475 °C evaluated  $\alpha'$  phase precipitation in non-equilibrium situation. The results calculated in Thermo-Calc were compared with experimental data.

### 3.2. X-Ray diffraction measurements

The  $\alpha'$  phase has the same crystal structure and lattice parameter similar to the ferritic matrix. Therefore, the XRD is not an appropriate technique to identify the  $\alpha'$  phase, but can be used to identify other secondary phases with lattice parameters and crystal structures different of ferrite.

Measurements of X-ray diffraction (Fig. 4) in aged samples at 400 °C for 1000 h revealed only the presence BCC phase and not identified the precipitation of intermetallic phases ( $\chi$ ,  $\mu$ ,  $\sigma$ ) under the conditions

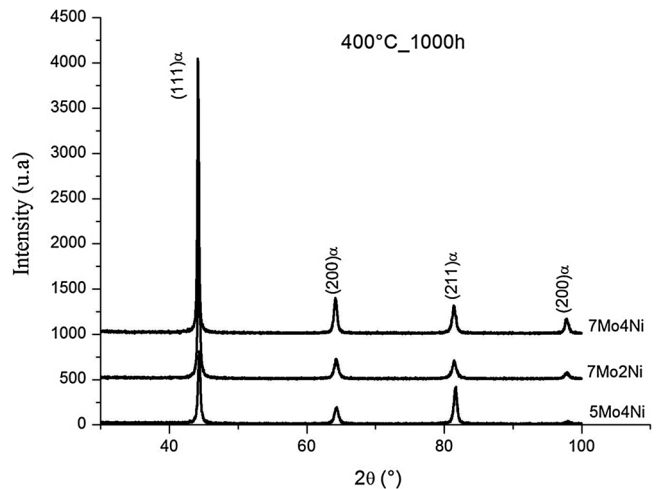


Fig. 4. XRD patterns to experimental alloys aging at 400 °C for 1000 h.

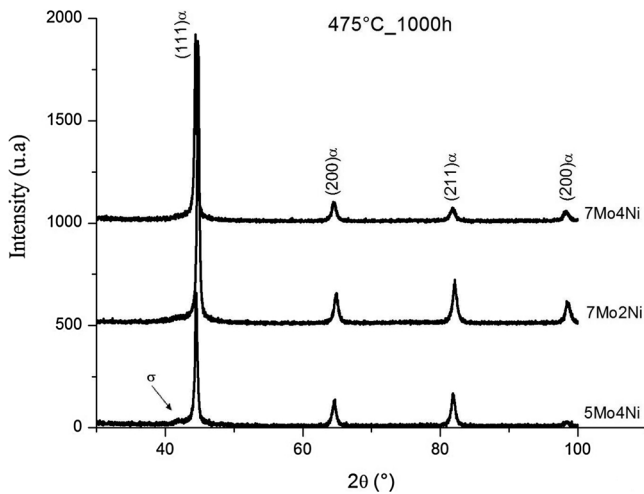


Fig. 5. XRD patterns to experimental alloys aging at 475 °C for 1000 h.

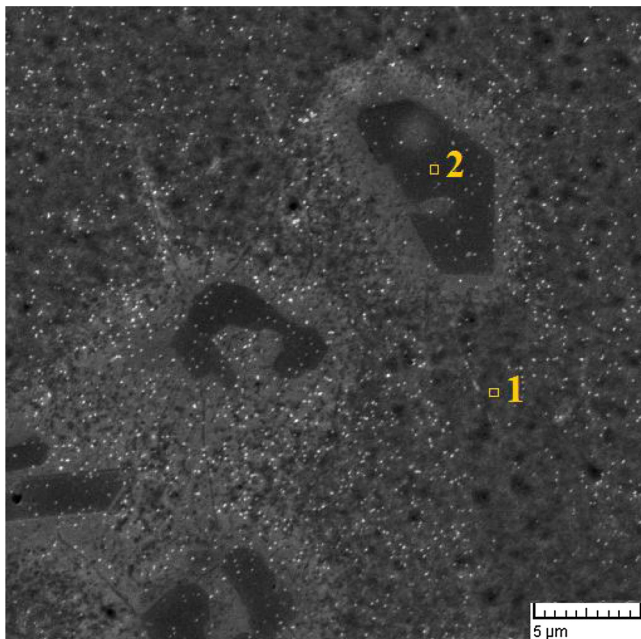


Fig. 6. SEM image of the 5Mo4Ni alloy aged at 475 °C for 1000 h.

studied. Although the diffractograms have not identified a second phase different of ferrite, according to the calculations of the Thermo-Calc  $\alpha'$  phase is more likely that temperature range and has the same crystal structure of ferritic matrix. Furthermore,  $\alpha'$  phase does not have molybdenum in its composition, is very thin and can not be observed by SEM or XRD [20–23].

The diffraction measurements were used in all samples, but the most relevant results were observed for the most critical situation of the 475 °C (1000 h), in the others time/temperature conditions the results were similar to those observed for the samples treated at 400 °C (1000 h).

Table 3

EDS measures (%mass) the points in the SEM image for 5Mo4Ni aged at 475 °C for 1000 h.

Points	%Cr	%Mo	%Ni	%Fe
1	24,78 ± 0,8	6,03 ± 0,4	4,23 ± 0,3	64,79 ± 1,9
2	62,86 ± 1,9	13,16 ± 0,7	2,2 ± 0,2	21,78 ± 0,8

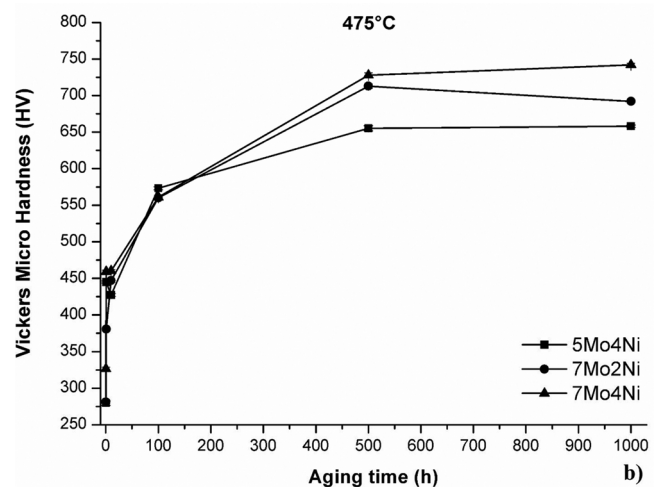
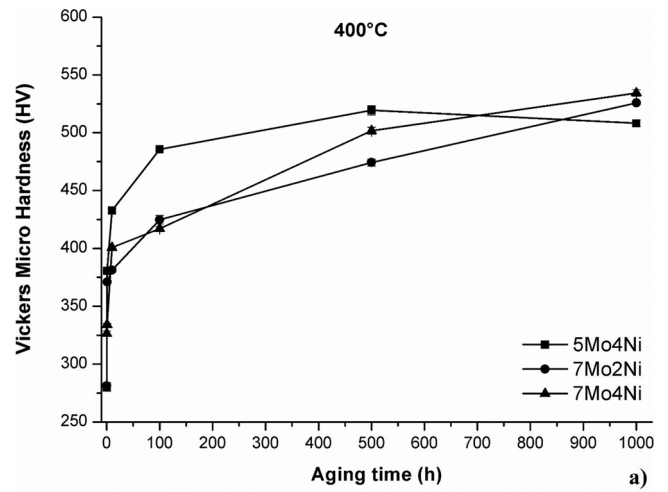


Fig. 7. Vickers micro hardness as a function of aging time for experimental alloys; a) 400 °C; b) 475 °C.

XRD patterns for samples with 7 wt.% of Mo aged at 475 °C for 1000 h only identified ferritic phase (BCC) peaks, whereas for the 5Mo4Ni alloy aged at 475 °C for 1000 h (Fig. 5), showed a very low intensity peak that does not correspond to BCC phase.

For 5Mo4Ni alloy treated at 475 °C it was compared the XRD patterns (Fig. 5) with SEM image (Fig. 6) and EDS measures (Table 3). The low intensity peak corresponds to Cr and Mo rich phase, showed in the SEM image (Fig. 6) for point (2) and identified with  $\sigma$  phase (about 62%Cr-13%Mo-2%Ni). The  $\sigma$  phase has tetragonal body centered (TBC) represented by  $(\text{Fe, Ni})_x(\text{Cr, Mo})_y$  with precipitation temperature range 500 °C a 1000 °C [26]. At 475 °C the  $\sigma$  phase precipitation is more likely than the precipitation of  $\chi$  phase (Precipitates rich in Mo) and chromium carbide ( $\text{M}_{23}\text{C}_6$ ), occurring in the superferritic stainless steels in the temperature range between 600 °C and 950 °C [4–7]. The point (1) was identified with ferritic matrix (about 24%Cr-6%Mo-4%Ni).

### 3.3. Mechanical and magnetic properties

The aging heat treatment led to an increase in hardness of the alloys (Fig.7a–b). For annealed samples micro hardness is in the range 280–380HV and increases with treatment time to about 620HV in 7Mo4Ni alloy treated at 475 °C for 1000 h. Changes in hardness of the alloys during aging were compared with the variation of the percentage of ferrite measured by a ferritoscope (Fig.8a–b). The increase in hardness was accompanied by a reduction in the ferritic phase.

The results from ferritoscope measurements (Fig.8a–b) showed a

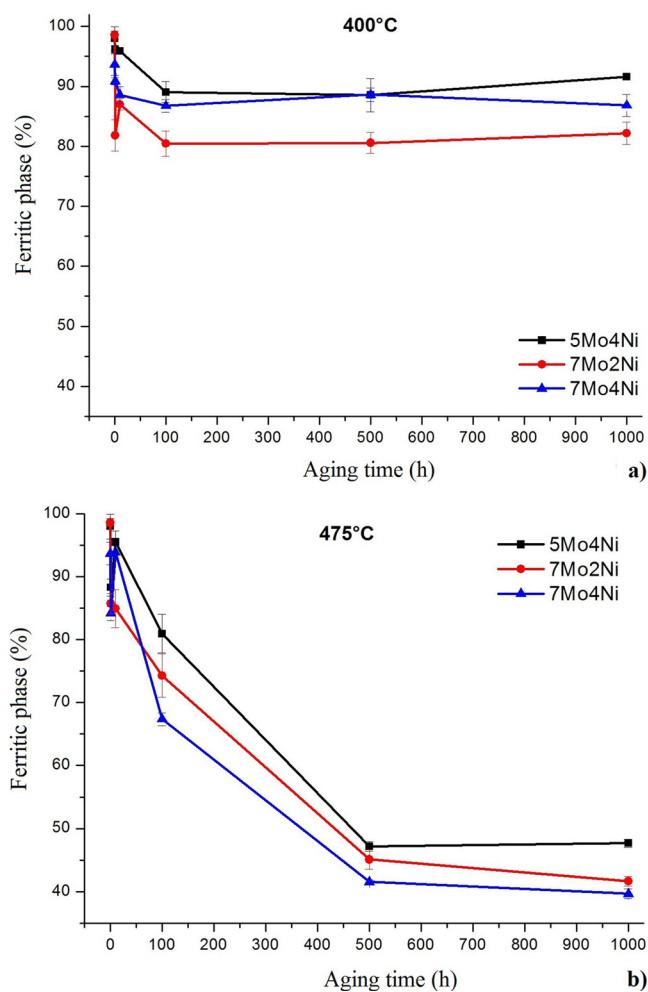


Fig. 8. Amount ferrite phase as a function of aging time a) 400 °C; b) 475 °C.

reduction of magnetic permeability on aged samples when compared to the solution annealed samples. The measurement obtained is proportional to the ferromagnetic phase content, i.e., ferritic phase.

Fig. 8 shows the change of ferrite phase with time at 400 °C (Fig. 8a) and 475 °C (Fig. 8b). The time less than one hour is the measure of annealed sample. The samples treated at 475 °C showed a greater reduction of the ferrite content in the samples treated at 400 °C. For the samples treated at 400 °C the reduction occurs until 100 h, reaching 80% in 7Mo2Ni alloy, remaining constant with increasing time. For samples treated at 475 °C for 500 h the amount of ferritic phase was approximately 40% in 7Mo4Ni alloy and 50% in 5Mo4Ni and 7Mo2Ni alloy and remains constant after 500 h. Other authors also observed the increase of the hardness related to the reduction of the ferritic phase in ferritic stainless steels aged in the same temperature-time range, this effect was attributed to the precipitation of a Cr-rich phase [20–23].

### 3.4. Corrosion analysis

Fig. 9 shows the anodic polarization curves for samples annealed and aged at 400 °C and 475 °C for 1000 h. It was measured the pitting potential ( $E_p$ ), corrosion potential ( $E_{corr}$ ), the passivation potential range ( $\Delta E_{pass}$ ) and passivation current density ( $i_{pass}$ ) for alloys presented in the Table 4. The higher potential indicates best corrosion resistance of the alloy. It was observed that annealed samples pitting potentials ( $E_p$ ) for 7Mo4Ni ( $E_p = 1,06$  V) and 7Mo2Ni ( $E_p = 1,04$  V)

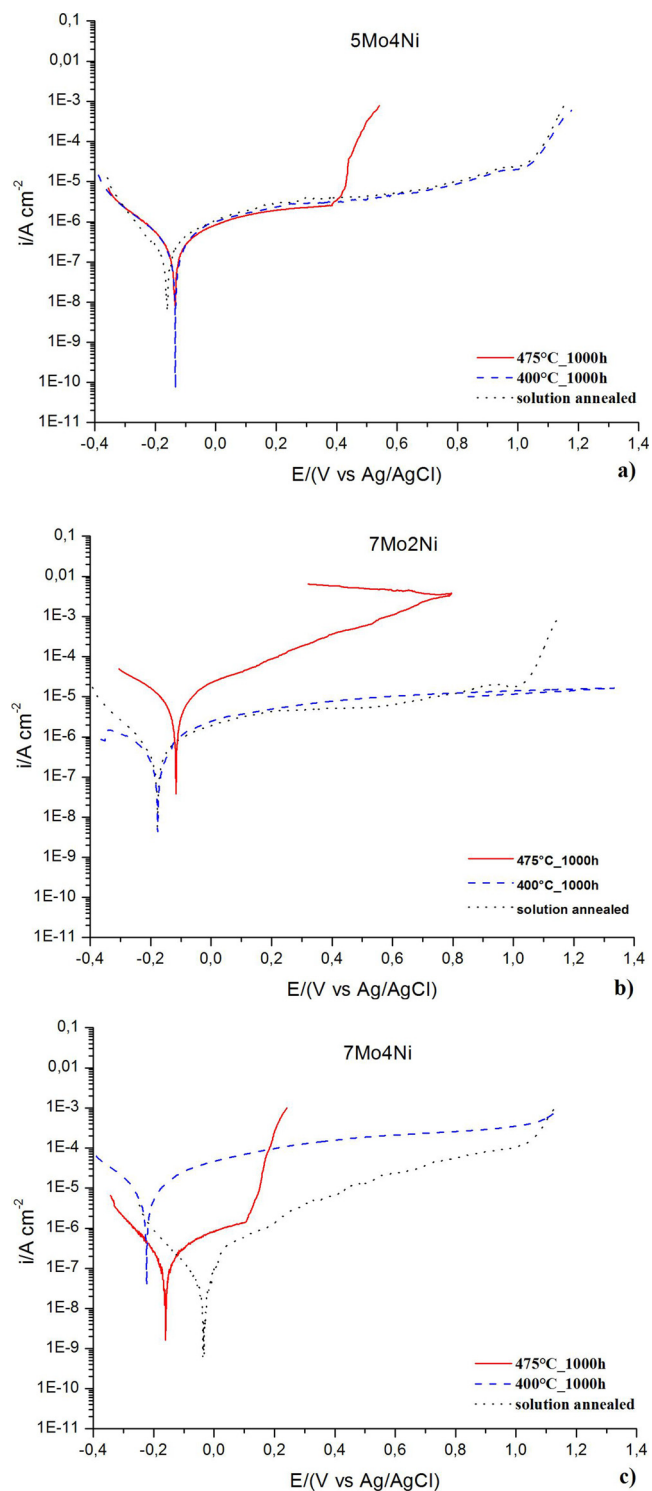


Fig. 9. Polarization curves for the solution and aging at 400 °C and 475 °C samples a) 5Mo4Ni; b) 7Mo2Ni c) 7Mo4Ni.

were greater than for 5Mo4Ni ( $E_p = 1,03$  V), probably due to the higher Mo content in these alloys. The increase Mo content in the FeCrMo alloys improve corrosion resistance in various environments [10–12].

For the samples treated at 400 °C for 1000 h, the pitting potential measurements remained the same measured for annealed samples between 1,03 V and 1,1 V. For alloys treated at 475 °C for 1000 h occurred

**Table 4**  
 $E_{\text{corr}}$ ,  $E_p$ ,  $\Delta E_{\text{pass}}$  and  $i_{\text{pass}}$  values extracted from the polarization curves.

Heat Treatment	Alloys	$E_{\text{corr}}$ (V)	$E_p$ (V)	$\Delta E_{\text{pass}}$ (V)	$i_{\text{pass}}$ ( $\mu\text{A}/\text{cm}^2$ )
Solution	5Mo4Ni	-0,16	1,03	1,10	3,10
	7Mo2Ni	-0,18	1,04	1,10	4,70
	7Mo4Ni	-0,04	1,06	0,95	12,70
400 °C 1000 h	5Mo4Ni	-0,14	1,04	1,03	3,0
	7Mo2Ni	-0,18	1,04	1,10	4,70
	7Mo4Ni	-0,22	1,06	1,06	62,2
475 °C 1000 h	5Mo4Ni	-0,14	0,40	0,40	2,10
	7Mo2Ni	-0,11	0,80	0,80	27,4
	7Mo4Ni	-0,16	0,10	0,10	1,20

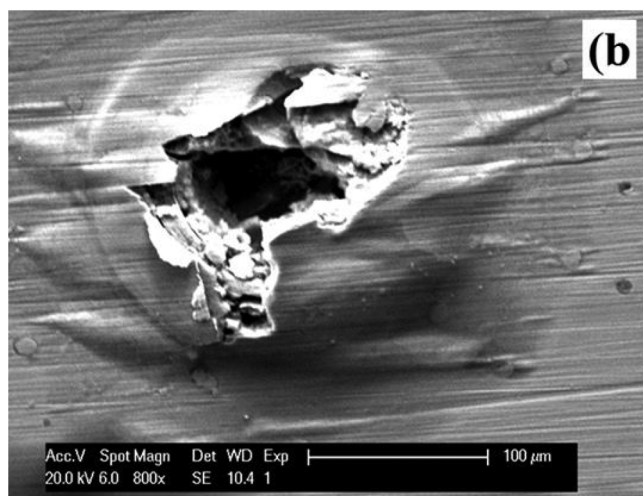
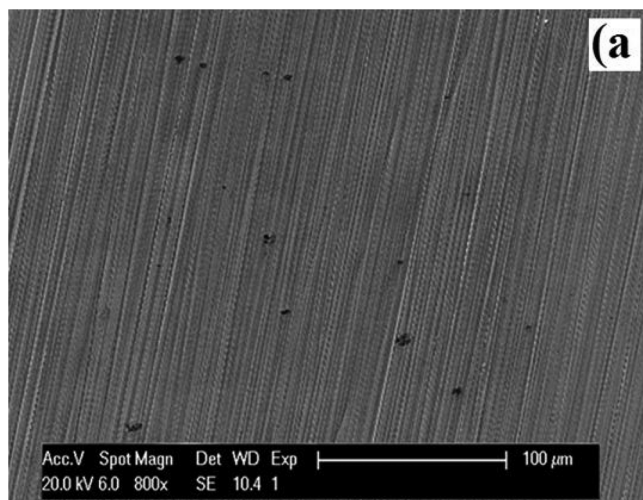


**Fig. 10.** SEM images of the surface after corrosion test for 5Mo4Ni alloy a) 400 °C\_1000 h b) 475 °C\_1000 h.

marked reduction of  $E_p$  to 0,1 V in 7Mo4Ni and 0,4 V in 5Mo4Ni. The thermal treatment at 475 °C for 1000 h also reduced the passivation

#### Appendix A

Eq. (1) The pitting resistance equivalent (PRE) number for stainless steels.

$$\text{PRE} = \% \text{Cr} + 3.3 (\% \text{Mo}) + 16 (\% \text{N}) \quad (1)$$

range ( $\Delta E_{\text{pass}}$ ) to about 1,03 V–0,4 V in 5Mo4Ni, 1,1 V–0,8 V in 7Mo2Ni and 0,95 V–0,1 V in 7Mo4Ni when compared to annealed samples and treated at 400 °C.

The heat treatment to 475 °C affects the resistance to pitting corrosion and passivation range, besides increasing the passivation current all alloys in relation to the solubilized state, these changes in the measured parameters showed instability of the passive film with reduced corrosion resistance and favor pitting corrosion. Comparing the results obtained in the corrosion test with the results of measurements of hardness and magnetic properties, the samples treated at 475 °C showed a reduction in corrosion resistance accompanied by an increase in hardness and a reduction in the amount of ferric phase. A higher amount of Cr-rich phase precipitated at 475 °C increased susceptibility to pitting corrosion in the Cr depleted matrix.

SEM (Fig.10) observed effects of corrosion on the surface of the aged and annealed samples. The surface of the alloy treated at 400 °C for 1000 h subjected to polarization test shows small pits as well as in annealed samples. While the corrosion test on the surface of the samples treated at 475 °C for 1000 h caused the formation of large amounts of pits due to brittle Cr-rich phase.

#### 4. Conclusions

According to Thermo-Calc calculations, Mo addition reduces the highest precipitation temperature for the  $\alpha'$  phase and increases the amount of this phase. While the Ni addition reduces the mass fraction of  $\alpha'$  phase precipitated. From the 450 °C temperature, in equilibrium conditions, it does not occur to  $\alpha'$  phase precipitation.

Experimental heat treatment at 400 °C and 475 °C for various times increased hardness of the alloys due to presence of a second hardest phase in the ferritic matrix. The diffraction patterns did not identify this phase, but confirmed that it is probably BCC as the matrix. The low intensity peak corresponds to Cr and Mo rich phase in the 5Mo4Ni alloy treated at 475 °C for 1000 h was identified as the most likely sigma phase. The use of ferritoscope revealed to be a good tool to study  $\alpha'$  phase precipitation. Measurements with it showed a decrease in magnetic permeability of alloys that can be related to the reduction of the ferrite (magnetic) phase caused by a paramagnetic phase, probably the  $\alpha'$  phase. The amount of paramagnetic phase precipitated at about 60% in the 7Mo4Ni aging at 475 °C for 1000 h. The effect of the presence of brittle phases on the corrosion resistance was more pronounced for samples treated at 475 °C for 1000 h. The alloys treated at 400 °C for 1000 h showed pitting potential approximately equal to that of the annealed sample. The surface of the samples treated at 475 °C after corrosion test showed that the formation of pitting corrosion was higher than in the samples treated at 400 °C and annealed, revealing the harmful effect on corrosion resistance due to the large amount of paramagnetic phase precipitated.

#### Acknowledgements

The authors wish acknowledge the financial support for research to FUNCAP (Fundação Cearense de Apoio ao Desenvolvimento Científico e Tecnológico). The authors would specially like to thank Mr. Oscar Gonzales, Metallurgist and Director of FAINOX (Fundição de aço inoxidáveis – São Paulo, Brazil) that kindly supplied the experimental super ferritic stainless steels used for this study.

## References

- [1] D. Janikowski, E. Blessman, Super-ferritic stainless steels – the cost-effective answer for heat transfer tubing, Proceedings of the Corrosion Conference, NACE, 2008.
- [2] C.W. Kovak, High Performance Stainless Steels, Nickel Development Institute (Cited 19 February 2016). Available from: (2011) [http://www.nickelinstitute.org/TechnicalLiterature/Reference%20Book%20Series/HighPerformanceStainlessSteels\\_11021.aspx](http://www.nickelinstitute.org/TechnicalLiterature/Reference%20Book%20Series/HighPerformanceStainlessSteels_11021.aspx).
- [3] P.A. Olubambi, J.H. Potgieter, L. Cornish, Corrosion behavior of superferritic stainless steels cathodically modified with minor additions of ruthenium in sulphuric and hydrochloric acids, *Mater. Des.* 30 (2009) 1451–1457.
- [4] T. Koutsoukis, K. Konstantinidis, E.G. Papadopoulou, P. Kokkonidis, G. Fourlaris, Comparative study of precipitation effects during aging in superaustenitic and super-ferritic stainless steels, *Mater. Sci. Technol.* 27 (2011) 943–950.
- [5] P.G. Ng, E. Clarke, C.A. Khoo, G. Fourlaris, Microstructural evolution during aging of novel superferritic stainless steel produced by the HIP process, *Mater. Sci. Technol.* 22 (2006) 852–858.
- [6] K.R. Chasse, P.M. Singh, Corrosion study of super ferritic stainless steel UNS S44660 (26Cr-3Ni-3Mo) and several other stainless steel grades (UNS S31603, S32101, and S32205) in caustic solution containing sodium sulfide, *Metall. Mat. Trans. A* 44 (2013) 5039.
- [7] N.J.E. Dowling, H. Kim, J.-N. Kim, S.-K. Ahn, Y.-D. Lee, Corrosion and toughness of experimental and commercial super ferritic stainless steels, *NACE* 55 (1999) 743–755.
- [8] I.P. Baptista, C.J.B.M. J6ia, et al., System and methodology for evaluating the naphthenic corrosivity in laboratory, In Portuguese, Conference on Equipment Technology. Proceedings of the 7th COTEQ Conference, (2003).
- [9] G. Gallo, J. Edmondson, The effect of molybdenum on stainless steels and naphthenic acid corrosion resistance, Proceedings of the Corrosion Congress, NACE, 2008.
- [10] L.B. Moura, R.F. Guimarães, et al., Naphthenic corrosion resistance, mechanical properties and microstructure evolution of experimental Cr–Mo steels with Mo content, *Mater. Res.* 15 (2012) 277–284.
- [11] M.J. Gomes da Silva, L.F.G. Herculano, A.S.C. Urcuzino, W.S. Araújo, H.F.G. de Abreu, P. de Lima-Neto, Influence of Mo content on the phase evolution and corrosion behavior of model Fe–9Cr–xMo (x = 5, 7, and 9 wt%) alloys, *J. Mater. Res.* 30 (2015) 1999–2007.
- [12] C.J. Park, M.K. Ahn, H.S. Know, Influence of Mo substitution by W on the precipitation kinetics of secondary phases and the associated localized corrosion and embrittlement in 29% Cr ferrite stainless steels, *Mater. Sci. Eng.* 418 (2006) 211–217.
- [13] N. Fujita, K. Ohmura, A. Yamamoto, Changes of microstructures and high temperature properties during high temperature service of niobium added ferritic stainless steels, *Mater. Sci. Eng.: A* 351 (2003) 272–281.
- [14] R.W.K. Honeycombe, H.K.D.H. Bhadeshia, *Steels Microstructure and Properties*, 3 Ed., (2006) 277–278p.
- [15] D.T. Llewellyn, R.C. Hudd, *Steels Metallurgy and Applications*, 3 Ed., Butterworth Heinemann, 1998 332–334p.
- [16] F.C. Pimenta Jr, W. Reick, A.F. Padilha, Comparative Study between Precipitation of the Sigma Phase in a Superferritic Stainless Steel and a Duplex Stainless Steel, In Portuguese 14 CBECiMat (Brazilian Congress of Materials Engineering and Science), São Pedro – SP, 2000, pp. 301–309.
- [17] D.M.E. Villanueva, F.C. Pimenta Jr, R.L. Plaut, A.F. Padilha, Comparative study on sigma phase precipitation of three types of stainless steels: austenitic, superferritic and duplex, *Mater. Sci. Technol.* 22 (2006) 1098–1104.
- [18] W. Xu, D. San Martin, P.E.J. Rivera Diaz del Castillo, S. Van Der Zwaag, Modelling and characterization of chi-phase grain boundary precipitation during aging of Fe–Cr–Ni–Mo stainless steel, *Mater. Sci. Eng.: A* 467 (2007) 24–32.
- [19] G. Kostorz (Ed.), *Phase Transformations in Materials*, WILEY-VCH, Germany, 2001.
- [20] O. Soriano-Vargas, E.O. Avila-Davila, V.M. Lopez-Hirata, N. Cayetano-Castro, J.L. Gonzalez-Velazquez, Effect of spinodal decomposition on the mechanical behavior of Fe–Cr alloys, *Mater. Sci. Eng.: A* 527 (2010) 2910–2914.
- [21] P.J. Grobner, The 885°F (475°C) embrittlement of ferritic stainless steels, *Metall. Trans.* 4 (1973) 251–260.
- [22] J.A. Souza, H.F.G. Abreu, A.M. Nascimento, J.A.C. Paiva, P. de Lima-Neto, S.S.M. Tavares, Effects of low-temperature aging on AISI 444 steel, *J. Mater. Eng. Perform.* 14 (2005) 367–372.
- [23] I.F. Vasconcelos, S.S.M. Tavares, F.E.U. Reis, H.F.G. Abreu, Ageing effects on  $\alpha'$  precipitation and resistance to corrosion of a novel Cr–Mo stainless steel with high Mo content, *J. Mater. Sci.* 44 (2009) 293–299.
- [24] J.M. Pardal, Superduplex Stainless Steel: Effects of Heat Treatments on Mechanical and Magnetic Properties and Corrosion Resistance, In Portuguese Blucher Acadêmico, São Paulo, 2012, pp. 216–218.
- [25] S.S.M. Tavares, J.A. Souza, L.F.G. Herculano, H.F.G. Abreu, C.M. Souza Jr., Microstructural, magnetic and mechanical property changes in an AISI 444 stainless steel aged in the 560 °C to 800 °C range, *Mater. Charact.* 59 (2008) 112–116.
- [26] W.F. Smith, *Structure and Properties of Engineering Alloys*, 2<sup>nd</sup> Ed., Mc.Graw-Hill, 1993.